Enhanced Pre-conditioning Algorithm for the Accurate Alignment of 3D Range Scans

Shane Transue and Min-Hyung Choi
Department of Computer Science and Engineering
University of Colorado Denver
Denver, CO, United States

Abstract – *The process of accurately aligning 3D range scans to reconstruct a virtual model is a complex task in generic circumstances. Yet by exploiting the data characteristics common to many mobile 3D scanning devices, we propose a two phase alignment solution that improves the alignment provided by the iterative closest point (ICP) algorithm. Current approaches target how the ICP algorithm aligns two range scans based on modifying minimization functions, sampling functions, and point correspondence techniques. However, while these approaches have provided subtle improvements in the alignment process, the ICP algorithm is still incapable of aligning low resolution range scans with very little overlap. Based on our proposed algorithm, we are able to increase the accuracy of the alignment provided by the ICP algorithm by 40% on low resolution scan pairs and we demonstrate the versatility of this approach by accurately aligning a variety scan pairs with small overlap regions.*

Keywords*: 3D scanning, range scan alignment, data filtering, object reconstruction, low-resolution scan alignment*

1 Introduction

The process of scanning physical objects to recreate virtual three dimensional models was once limited from widespread adoption due to costly hardware components and sophisticated reconstruction techniques required to produce a final model. However recent developments in mobile laser based scanning devices have eliminated these barriers in the domain of long range, low resolution object reconstruction. While there has been extensive research into the alignment of high resolution scans from devices with limited range, only a select few target the long range, low resolution scans that are associated with long range, laser based scanning devices. Based on these developments we propose an algorithm that aids existing alignment algorithms for the reconstruction of a virtual model given a very limited set of low resolution scans. We build on the extensive existing developments in range scan alignment algorithms to utilize the characteristics of low resolution laser based scanning devices to present improvements in exiting alignment techniques for datasets that exhibit these characteristics.

In this paper we provide a detailed process pipeline that culminates with a robust approach to providing highly accurate pair-wise alignments between range scans constructed with low resolution scanning devices. In Section 2 we present previous research in pair-wise scan alignment and we reflect on how our proposed approach works in cooperation with these existing developments. In Section 3 the characterizations of the targeted laser scanning devices are defined and a technical overview of the scanning process for these types of scanners is presented. Section 4 develops a set of robust range scan cleaning tools that allow for the automated and manual elimination of background data and outliers from collected scans. As a prerequisite for our proposed algorithm, Section 5 details an accurate initial alignment of all generated scans to provide a rough alignment that attempts to reconstruct the object's surface. Utilizing this approximate reconstruction we present our alignment algorithm that provides a highly accurate alignment between scans with very little overlap. Our proposed approach is extensively tested on a wide variety of datasets and it is demonstrated that our approach decreases the pair-wise alignment error provided by using a naïve alignment algorithm by approximately 40 percent.

2 Related Work

The process of performing a pair-wise alignment on a set of range scans is well studied and numerous alternative techniques have been proposed to improve the efficiency and accuracy of this process. Namely, the iterative closest point (ICP) algorithm proposed by Besl and McKay [1], has spurred the development of several variants that support additional approaches [2] to how their ICP algorithm is performed. These developments aim to improve the quality of the results obtained through this pair-wise alignment approach. These techniques target specific modular aspects of the ICP algorithm such as the error function, the form of sampling used, and alternative schemes for matching corresponding points between the overlap regions of the scans.

Torsello et al. [3] propose a method of selecting relevant points from individual scans with the intent of improving the alignment through feature based point selection as a variant of the sampling used for the ICP algorithm. The critical aspect of our development is that our method is algorithmically orthogonal to these developments that define on what basis the ICP algorithm provides an accurate alignment. Since this is the case, this improvement can be used in cooperation with our approach, thus providing an extended toolset for the

process of rapidly aligning low resolution range scans, specifically those with minimal overlap regions.

Frank B. ter Harr and R.C. Veltkamp [4] propose a multi-view alignment scheme based on four scans which contain small overlap regions. However, this method does not target the low resolution scans obtained by most pan and tilt based time-of-flight (TOF) devices. Based on the complexities in this approach, alignment time is in the order of minutes for high resolution scans. In contrast, we are specifically targeting mobile devices and based on this requirement we present a series of algorithms that align similar high resolution scans in the order of milliseconds, thus making the alignment of lower resolution scans trivial. From this development we can than target mobile devices for the efficient alignment of low resolution scans.

A similar object reconstruction pipeline is proposed by Chatterjee et al. [5]. However, they rely on a high number of scans (~16) to reconstruct the surface of an object. In contrast, our objective is to minimize the total number of scans and we present an object reconstruction pipeline that facilitates this.

Unlike other approaches that rely on additional color information [6] in addition to distance measurements, we target TOF devices that only provide depth images to define an objects surface. By limiting our algorithms to perform only on depth information we target a larger range of TOF devices, specifically those without color or texture information.

Considering these prior developments, we propose that our algorithm can be utilized with any improvements of the ICP algorithm to increase the accuracy of our alignment. Our approach simply provides the consolidation of previous alignment techniques utilized by the ICP algorithm with an estimated selection of points contained in overlap regions. Based on these factors we improve the alignment provided by the ICP algorithm for scan pairs with small overlap regions.

By utilizing the ICP algorithm for a refined alignment, we extensively evaluate this proposed technique by statistically analyzing the root mean square deviation (RMSD) error produced by the naïve ICP alignment algorithm versus our proposed algorithm. This provides a well known basis upon which we can objectively evaluate the accuracy of the alignments performed by both algorithms for various datasets. Our evaluation is combined with some of the efficient variants of the ICP algorithm to provide robust and highly accurate alignment results. Specifically, the evaluation of our proposed algorithm utilizes uniform norm-space sampling and the point-to-plane variant proposed by Chen and Medioni [7] implemented by the Scanalyze package [8].

3 Scanning Device and Process

In this section the laser based scanning device and its data characteristics used in the development of our approach is declared and a detailed outline of the required scanning process is presented. The objective we propose is the reconstruction of a relatively large object such as a piece of furniture or a vehicle through the collection of range scans. This is performed with a laser based device around the object from various angles. In this context we refer to the reconstruction of the object as the process of collecting a set of scans from around the object and then aligning these consecutive scans to effectively model the object in 3D space. This process is accomplished through the use of a scanning device that is capable of measuring depth information at various locations on the target object's surface.

Specifically, we look at the use of a laser based TOF device to capture the surface information of a targeted object. The laser based TOF device is designed to construct a range scan through the use of two basic functions: tilt and pan. Using this basic functionality, the range scan captured by the TOF device is stored into a 2D array and is defined by five parameters: the position of the device P, n the number of tilt rows in the scan, m the number of columns, the pan range $(-\theta, \theta)$, and the tilt range $(-\phi, \phi)$. An abstract representation of the scan volume constructed by these parameters is illustrated in Figure 1. and each position in the 2D array corresponds to a single distance measurement between the scanner at position P and the surface of the target object.

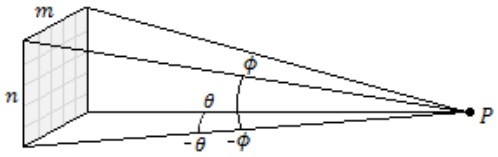

Figure 1. TOF Tilt-Pan Scanning Device

Utilizing this type of scanning device we construct the surface of the object, subject to the mobility limitations of the device. For the case of stationary tilt-pan laser scanners, this limits the movement of the device such that its position P moves coplanar to the ground around the object being scanned (specifically we utilized a tripod with adjustable tilt and elevation with a mounted TOF device). Given these constraints the surface of the object is defined by collecting a set of scans from various angles, counter-clockwise around the target object. Figure 2. illustrates this scanning procedure as seen from a top-down view:

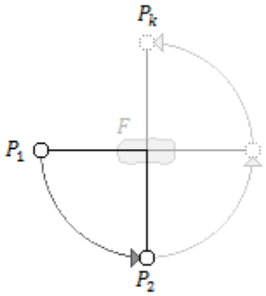

Figure 2. Tilt-Pan Device Scanning Procedure (Top-Down View)

Arbitrarily assigning some position as the starting position P_1, a set of scans is collected around the target object F. Each time a scan is captured, the device is moved to the next position where $P \in \{P_1, P_2, \ldots, P_k\}$ for k scans. Since position P_1 is the first scan we label this as scan as the 0° scan. For the next position (in Figure 2) at P_2 the scanner has been moved by 90° around the object. We label this scan as

the 90° scan, and so on. This is continued for every scan performed around the object where $0° \leq angle \leq 360°$.

In our datasets, we consider two scan set sizes: 4 and 8. When we consider a scan set (also called a scan batch) of 4 scans this typically means that the scans were performed close to the following angles: $\{0, 90, 180, 270\}$ where the scanner was moved around the object by 90° after each scan. Similarly when we consider a scan batch with 8 scans, they are typically performed in 45° increments around the target object: $\{0, 45, 90, 135, 180, 225, 270, 315\}$. The angle value for each scan is provided by the user and used to apply the appropriate rotation to each scan during the reconstruction process. The user must estimate the approximate angle at which they are performing each scan. If the user is within ~10° of the actual angle, the construction is unaffected.

4 Automated Filtering and Painting

Scan data collected by a tilt and pan based TOF scanning device typically includes a lot of additional unnecessary information about the environment in which the target object resides. This background information is usually unintentionally included in the scan data and does not contribute to the surface definition of the object we are interested in reconstructing. Specifically, we identify any point that does not directly contribute to the definition of the surface of the target object as background information. The separation of these points from those that define the surface of the target object is handled through two phases (1) automated filtering and (2) manual data elimination painting.

Automated filters remove background information based on the TOF device parameters and the data collected from the device, and can be used to quickly eliminate a majority of the background information contained in a scan. Based on the characteristics of a tilt and pan TOF device, the following set of filters can be adopted: distance filters, signal strength filters, and filters based on the intervals for which the pan angle θ and tilt angle ϕ are valid. Providing these automated filters allows the target object to be easily cropped from its surrounding environment. This technique, however, does not address background information collected between complex surfaces as demonstrated in Figure 3. (center). Surfaces with complex material properties (such as transparency) cannot always be accurately removed with an automated process.

To address surfaces with complex material properties we provide a highly accurate data elimination painting tool. Based on the 3D to 2D projection of the individual points contained in the scan data, a radial painting tool can be used to carve out additional unnecessary data points. This allows for an extremely accurate representation of the objects surface to be extracted at the cost of manual intervention. However, based on the simplicity of the developed toolset, we illustrate the quality of a surface that can be extracted from a 90° scan of a vehicle using this manual technique after ~10 minutes of manual painting as shown in Figure 3. (right). This allows for the extraction of the target object which is required for the accuracy of the bounding volumes calculated in our proposed initial alignment algorithm that estimates the translations required to reconstruct the surface of the target object.

Figure 3. Unmodified Raw Data (left), Auto-Filtered Data (center), Manual Painting-Based Data Elimination (right).

5 Initial Alignment

When utilizing the ICP algorithm to perform a pair-wise alignment, a requirement of the algorithm is a rough initial guess alignment that provides an adequate starting position for each scan before their point distances are minimized. Thus, this process is a direct prerequisite for our highly accurate modified ICP algorithm. Again, we utilize the characteristics of the data provided by a pan and tilt TOF device. Specifically this allows us to consider a limited domain in which scans need to be properly aligned to reconstruct the surface of the target object. From Section 3, we note that the rotational value for each scan has been provided by the user within some error threshold. These rotations are applied to each scan to rotate them about the Y axis (the axis perpendicular to the ground upon which the scanning device sits). This provides the correct rotation for each scan as shown in Figure 5. (top row). However, a proper translation between each of the scans is required to accurately estimate an initial alignment that reconstructs the object's surface.

There are two aspects of this initial alignment scheme that dictate the quality of the alignment produced. First, the provided data must be properly rotated to match the scanning pattern performed around the object. Second, the point cloud data constructed from the scan information must not contain any outliers. Specifically, axis-aligned bounding boxes (AABB) are utilized to determine how much each scan must be shifted to accurately represent the objects surface. Therefore, the amount of error introduced by an outlier in the calculation of the AABB will significantly contribute to the misalignment of the scans in the batch; however, if both of these prerequisites can be fulfilled and a tilt and pan TOF device is used, an accurate estimation of the object's surface can be constructed efficiently.

In this section, we propose an efficient algorithm that determines the translations required to align two portions of a single surface contained in two consecutive scans. The idea behind this algorithm is that since we are utilizing a device that can only be moved around the target object in one plane, we can exploit that characteristic to provide a rough alignment of all scans in a batch with an efficient rough alignment algorithm. This rough alignment can then be used as a suitable initial alignment required by our proposed bounding volume assisted ICP algorithm.

Algorithm Description: Given a set of scans, each with an associated user provided angle that signifies the position of the scanner around the target object, rotate each scan about the *Y* axis and calculate the translation required to move each scan such that the surface contained in the scan's AABB is aligned with the previous scan in the batch.

From the provided scan batch we consider two scans at a time and define the user provided angle of the first scan as Θ and the angle of the second scan as Φ. We also define a Cartesian plane with four quadrants $(0-3)$. Since the scans AABBs reside in this plane, each of the four corners of each AABB correspond to the same quadrant labels. This scheme is used to determine how to shift one scans position to another based on their AABB extents.

We calculate the quadrant that has the highest percentage overlap based on Θ and Φ. This is illustrated in Figure 4. (left), where quadrant 0 has the highest percentage of overlap between the two scans. This indicates that scan two will be shifted to the first scan's position so that quadrant 0 of both AABBs coincide. This is illustrated in Figure 4. (center). This top-down view presents the AABBs of two individual scans before the initial alignment is performed. Since quadrant 0 has the highest amount of overlap for these two angles, it is selected and the AABB of scan two is shifted to the AABB of scan one (the upper right-hand corner).

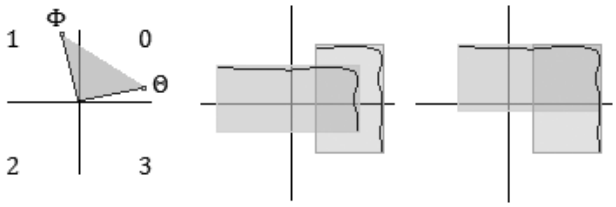

Figure 4. Quadrant Overlap for two Scans (left), initial scan positions (center), AABB aligned scans (right).

Input: A set of point clouds $P = \{P_1, \dots, P_n\}$, A set of user provided angles A, where $|A| = |P|$, $0 \le a_i \le 360 \ \forall a \in A$, and a_i corresponds to p_i where $p_i \in P$.
Output: The modified set of point clouds P, where each scan is translated so that every scan approximates its appropriate portion of target object's surface.

Algorithm: Pair-wise AABB Translational Alignment
0 Sort P by angle $(p_1.angle \le \cdots \le p_n.angle)$
1 Translate each point cloud to its geometric centroid
2 For each pair of scans: $\{p_1, p_2\}, \{p_2, p_3\}, \dots, \{p_{n-1}, p_n\}$
3 $\theta = p_i.angle$
4 $\phi = p_{i+1}.angle$
// Calculate quadrant with highest overlap %
5 $quad$ = HighestOverlap(θ, ϕ) // Figure 4. (left)
6 $aabb_i = AABB(p_i)$
7 $aabb_{i+1} = AABB(p_{i+1})$
// Figure 4. (center, right) Translation t
8 t = Shift $aabb_{i+1}$ to $aabb_i$ based on the selected $quad$
9 Apply t to point clouds $p_{i+1}, \dots, p_n$

With the batch sorted by scan angle, each pair of scan angles are analyzed to determine what quadrant contains the highest overlap. Once the shift direction (quadrants $0-3$) is determined by this analysis, the AABBs of the two scans are calculated to determine the translation required to move $aabb_{i+1}$ to $aabb_i$.

The results of this algorithm are demonstrated through its application to various datasets and are illustrated in Figure 5. (bottom row). Three diverse scan batches are considered for the demonstration of this algorithm: the Stanford bunny model provided by the Stanford Scanning Repository [9], the Subaru Legacy dataset obtained from a pan and tilt TOF device, and a Toyota truck model constructed through the use of a virtual scanner developed to emulate the data collected from a pan and tilt TOF device.

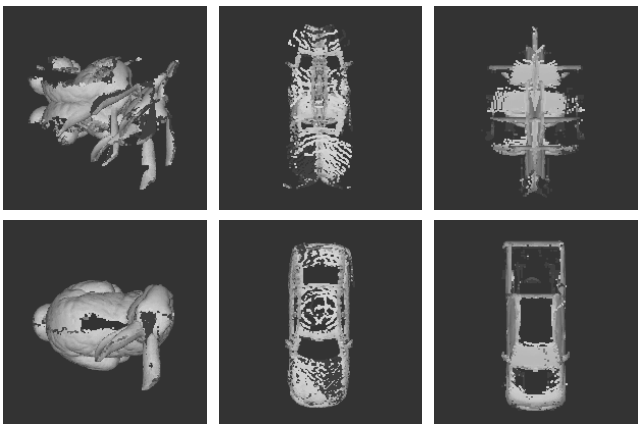

Figure 5. Initial Alignment performed on the Stanford Bunny (left), Subaru Legacy (center), and virtual Toyota Truck (right) datasets.

The results in Figure 5. (bottom row) demonstrate the accuracy of this approach. This is required by the bounding volume assisted ICP algorithm because it specifically targets overlap regions between scan pairs. Without this accurate initial alignment, our proposed method may not select the best overlap regions corresponding to each scan pair.

6 Bounding Volume Assisted ICP

In this section, we present an efficient way of improving the alignment between two scans that contain minimal overlap. Since we are utilizing a pan and tilt based TOF device to reconstruct a physical object, it is desirable to minimize the total number of scans required to accurately construct the entire surface of the object. However, limiting the number of scans performed dictates that between every scan pair, the overlap region is greatly reduced. This poses a challenge for the ICP algorithm, which operates under the assumption that there is a significant overlap region in common between both scans. Here we provide a method of extracting this overlap region and utilize the ICP algorithm to align the points that are contained in this volume. Therefore, the resulting alignment between the points in this volume will increase the accuracy of the alignment due to the high level of correspondence between the point sets.

In our alignment process, we aim to accurately calculate the overlap region shared between two scans. To do this, we utilize the accuracy of the initial alignment, provided in the previous section, to provide an efficient way of calculating this overlap region using bounding volumes. Since we are using a tilt and pan TOF device with limited mobility, we exploit this simplicity and use AABBs to represent the bounding volumes that will be used to calculate this overlap between scan pairs. This is performed by constructing AABBs for each scan and then calculating the AABB that represents their intersection. Once this intersection volume is defined, two sets of points are constructed (1) P_a, the points from the source scan that are contained in the intersection volume and (2) P_b the points from the target scan that are contained in the intersection volume. The ICP algorithm is then used to align these two point subsets from the original scans. Once the transformation is calculated by the ICP algorithm, it is simply applied to the source scan so that it is properly aligned to the target scan. This results in an improved alignment between the two scans with very little computational overhead, which is ideal for mobile scanning solutions.

Algorithm Description: Given a set of scans featuring a low percentage of pair-wise overlap, perform an ICP alignment between each pair of scans utilizing only the points that exist in their overlap region. The algorithm is provided in terms of abstract volumes.

Input: A set of point clouds $P = \{P_1, \dots, P_n\}$
Output: The modified set of point clouds P, where each scan is aligned to the previous scan in the set.

Algorithm: Pair-wise AABB Assisted ICP Alignment
0 For each pair of scans: $\{p_1, p_2\}, \{p_2, p_3\}, \dots, \{p_{n-1}, p_n\}$
1 $v_i = Volume(p_i)$
2 $v_{i+1} = Volume(p_{i+1})$
3 $intersection = v_i \cap v_{i+1}$
// Collect the point subsets from each scan
4 For every point $p \in P_i$
5 $P_a += p$ iff $p \in intersection$
6 For every point $p \in P_{i+1}$
7 $P_b += p$ iff $p \in intersection$
// Perform the ICP algorithm between P_a and P_b
8 $t = ICP(P_a, P_b)$
9 Apply t to P_{i+1}

In this algorithm, the intersection between the volumes associated with each scan is calculated, followed by the construction of two sets: P_a and P_b that will be used for the ICP alignment. The sets P_a and P_b contain points from the source and target scan respectively if and only if the points are contained in the intersection volume: $intersection$. The resulting transformation t is then applied to the source scan P_{i+1}. This is performed for each pair contained in the set, thus upon completion, when the ICP algorithm converges, the target object should be accurately reconstructed.

Figure 6. illustrates how this algorithm is applied to scan pairs during the alignment process. This illustration also demonstrates that based on our accurate initial alignment, we can determine the overlap areas that correspond to each scan.

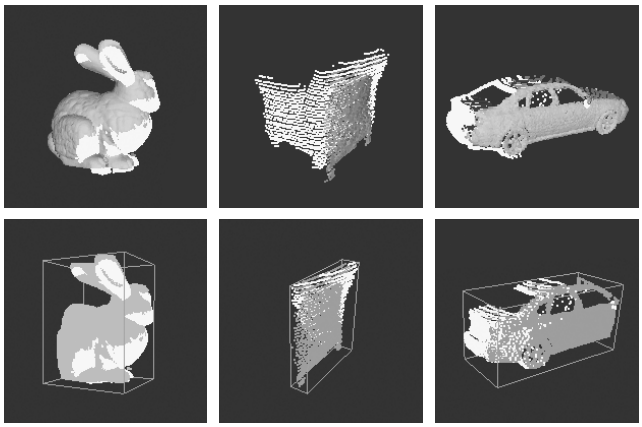

Figure 6. AABB Intersections between Scan Pairs for the Stanford Bunny (left), Chair (center), and Subaru Legacy (right) datasets.

The (top row) of Figure 6. displays two scans (where one is selected in white and the other is default gray), with an initial alignment performed. The (bottom row) of Figure 6. displays the intersection AABB calculated between the AABBs of each scan and the point sets P_a and P_b are shown in default gray and white respectively. These are the two point sets that are aligned using the ICP algorithm.

Based on this alignment scheme the overall alignment error between two scans with very little overlap is reduced thus allowing for a minimal number of scans (~4) to provide enough information to reconstruct an object. Figure 7. shows the results of this approach for the Stanford Bunny, the Subaru Legacy, Chair, and Virtual Toyota Truck scan sets.

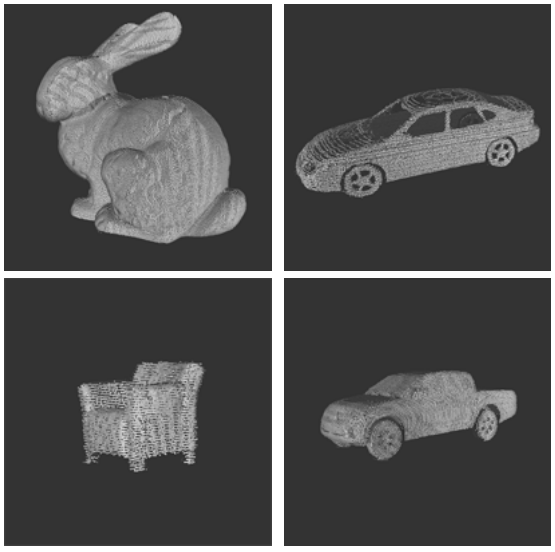

Figure 7. Results of the AABB-Assisted ICP Alignment for all four datasets. Stanford Bunny (upper left), Subaru Legacy (upper right), Chair (lower left), and Virtual Truck (lower right).

7 Experimental Evaluation

In this section, it is shown that the proposed bounding volume assisted ICP algorithm yields better results for low overlap scan pairs in various datasets. These datasets are provided from three independent sources: the Stanford 3D Scanning Repository (Stanford Bunny), a pan and tilt based TOF device, and the virtual scanning device developed to emulate a pan and tilt TOF device (without distance measurement error). The application of the proposed algorithm to this diverse set of datasets illustrates the robust capabilities of the proposed algorithm in this domain. The ICP algorithm implementation from the Scanalyze package is utilized to perform all preceding tests. Specifically, from this implementation we utilize uniform normspace-sampling, with a point-to-plane minimization function.

For each test performed, we use the initial alignment algorithm provided in Section 5. to provide a starting position for each scan in a batch. This ensures that both our proposed algorithm and the ICP algorithm can rely on the same initial conditions prior to alignment. The limited set of parameters, modified depending on the overlap contained in each dataset for the ICP algorithm, are show below:

ICP Parameters

Sampling Rate: 0.20
Iterations: 10
Minimization: Point-to-Plane
Uniform Normspace Sampling
Culling Percentage: Based on pair-wise overlap
  20 for scan batches containing 8 scans
  50 for scan batches containing 4 scans
AABB Inflation*: 10%

* For datasets provided from a TOF scanning device that contain distance measurement errors we provide an artificial AABB inflation percentage for our proposed method to handle these erratic samples.

The results in Figure 8. and 9. illustrate the convergence of the two algorithms over the course of 10 iterations using the settings provided above for the Stanford Bunny and Legacy batches. Each of these batches contains four scans, each separated by 90°. The average RMSD collected over 10 repeated batch alignments is shown for the alignment between the 180° – 270° scans of both batches.

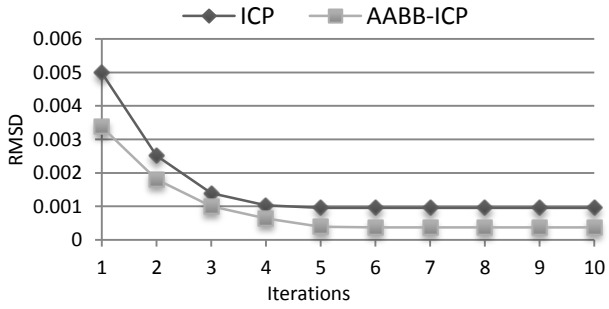

Figure 8. Stanford Bunny 180°-270° Scan Alignment RMSD

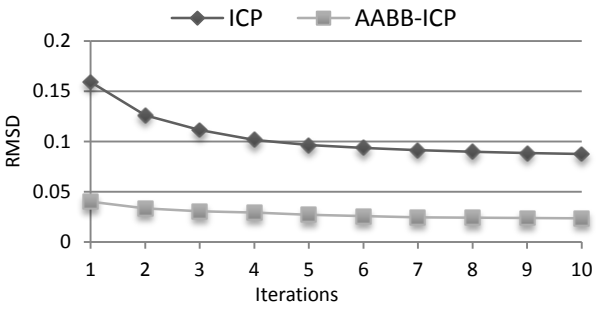

Figure 9. Subaru Legacy 180°-270° Scan Alignment RMSD

From these results, we observe that the AABB assisted ICP algorithm converges with a lower RMSD error than the unassisted ICP algorithm. We see a large discrepancy in RMSD error between the Stanford Bunny (Figure 8.) and Subaru Legacy (Figure 9.) datasets due to the vast resolution difference between these objects. However, both alignments improve upon the naïve ICP alignment by reducing the pair-wise RMSD, thus providing a more accurate alignment. We show this result is constant for all scan datasets by evaluating the RMSD error reduction percentage provided by the AABB-ICP algorithm over the naïve ICP algorithm for all available datasets.

Utilizing the same ICP settings and initial alignment as before, we evaluate the alignment performance between each algorithm for the datasets containing 8 scans. For these batches each scan pair is only separated by 45°. Figure 10. shows the percent decrease in RMSD for the AABB assisted algorithm versus the naïve ICP algorithm for these scans with approximately 50% overlap between each scan pair.

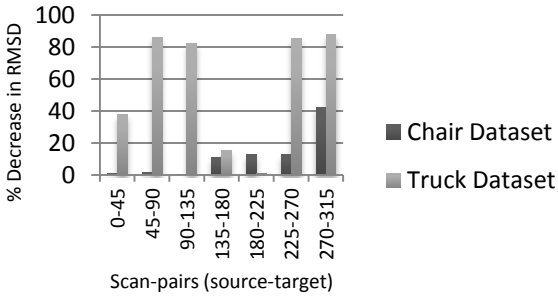

Figure 10. % Decrease in RMSD provided by the AABB assisted ICP algorithm [vs] the naïve ICP algorithm for batches with 8 scans.

While the proposed algorithm provides improvements in the alignment quality, the result varies dramatically due to the high overlap shared between each of these alignments. Since the scan pairs considered in these batches contain large overlap regions, the performance can degrade to that of the naïve ICP algorithm due to the large number of points selected for alignment from both scans.

Our approach, however, is specifically targeted at scan pairs with smaller overlap regions; therefore, we conduct the same test on the scan batches that only contain 4 scans. Each of the scans in these datasets are separated by 90° as stated

before. This provides a very limited overlap region for each algorithm to use to find the proper correspondence between scan pairs. Figure 11. shows the results of this test.

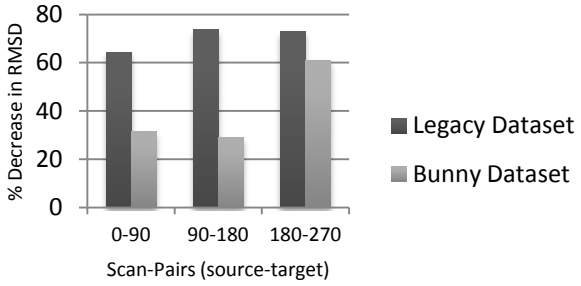

.

Figure 11. % Decrease in RMSD provided by the AABB assisted ICP algorithm [vs] the naïve ICP algorithm for batches with 4 scans.

The results we observe from the alignment of the scan batches containing 4 scans is that the AABB assisted ICP algorithm provides a consistent improvement in the accuracy of the alignment between scan pairs. Thus, this algorithm can be utilized to yield a better alignment than the naïve ICP algorithm.

8 Conclusion and Future Work

In this paper, we presented a two phase solution that improves the accuracy of the alignment provided by the ICP algorithm by approximately 40 percent. By exploiting the device characteristics common to most 3D scanning devices, including TOF devices, we have provided an extensive set of tools that can be utilized to ensure that the ICP algorithm converges, even for low resolution scan sets with small overlap regions. We also effectively illustrated that our approach can be utilized with existing variants of the ICP algorithm that improve the quality of the alignment between scan pairs as stated in Section 2. Sections 3 and 4 illustrated the process of collecting and editing scan data as the pre-processing steps required for our alignment algorithm. Sections 5 and 6 provided detailed descriptions of our two phase algorithm and formed a basis upon which we can evaluate this alignment approach. In Section 7, we presented two common ICP configurations that were effectively used to determine the decrease in RMSD provided by the second phase of our algorithm compared to using an ICP algorithm that tries to determine a correct alignment using all available points from both scans.

In our future work, we would like to address the requirement placed upon the user to provide the angle of each scan during the scanning process. By exploring the possibility of estimating the scanner position, we would like to remove this requirement by estimating this rotational value from the estimated scanner positions. We would also like to explore the possibilities of creating a fully automated filtering process to remove the manual editing requirement from our pre-processing as well. In this paper we think that we have contributed to the process of accelerating the adoption of mobile scanning devices and we would like to see these technologies made widely available for all purposes. We hope that by developing this two phase alignment algorithm we can simplify the process of reconstructing a physical object from range scan sets.

9 References

[1] Paul J. Besl, and Neil D. McKay. "A Method for Registration of 3-D Shapes". IEEE Transactions on Pattern Analysis and Machine Intelligence (PAMI), 14(2), pp. 239–256, 1992.

[2] Szymon Rusinkiewicz and Marc Levoy. "Efficient Variants of the ICP Algorithm". Proceedings of the International Conference on 3-D Digital Imaging and Modeling (3DIM), pp. 145–152, 2001.

[3] Torsello, A.; Rodola`, E.; Albarelli, A., "Sampling Relevant Points for Surface Registration," 3D Imaging, Modeling, Processing, Visualization and Transmission (3DIMPVT), 2011 International Conference on , vol., no., pp.290,295, 16-19 May 2011.

[4] ter Haar, F.B.; Veltkamp, R.C., "Automatic multiview quadruple alignment of unordered range scans," Shape Modeling and Applications, 2007. SMI '07. IEEE International Conference on, vol., no., pp.137,146, 13-15 June 2007.

[5] Avishek Chatterjee, Suraj Jain, and Venu Madhav Govindu. "A pipeline for building 3D models using depth cameras". ICVGIP '12 Proceedings of the Eighth Indian Conference on Computer Vision, Graphics and Image Processing. Article No. 38, 2012.

[6] Shen Yang, Yue Qi, Fei Hou, Xukun Shen, and Qinping Zhao. "A novel method based on color information for scanned data alignment". Proceedings of the 2008 ACM symposium on Virtual reality software and technology, pp. 201-204, 2008.

[7] Yang Chen, and Gerard Medioni. "Object Modeling by Registration of Multiple Range Images". International Journal of Image and Vision Computing, 10(3), pp. 145–155, 1992.

[8] Scanalyze: A System for Aligning and Merging Range Data. http://graphics.stanford.edu/software/scanalyze/

[9] Stanford 3D Scanning Repository http://www-graphics.stanford.edu/data/3Dscanrep/